JOURNAL OF MATERIALS SCIENCE 28 (1993) 4366–4374

# Diffusion bonding of a nickel (chromium) alloy to zirconia: mechanical properties and interface microstructures

C-D. QIN, B. DERBY
*Department of Materials, University of Oxford, Oxford, OX1 3PH, UK*

Diffusion bonding of a Ni(Cr) alloy with $ZrO_2$ has been studied. It was found that the processes were controlled by chemical reactions at the metal/ceramic interface forming compounds within the composition range $NiO_{1-x}Cr_2O_{3-y}ZrO_{2-z}$ $(0 < x,y,z < 1)$. Reaction products were characterized by examination of the fractured metal/ceramic halves and from cross-sections using optical, scanning and transmission electron microscopy and energy dispersive X-ray microanalysis. These metallographic studies indicate that the interface reactions are accompanied by local melting indicating a possible eutectic reaction following interdiffusion. Pre-oxidizing the metal foil enhances these reactions and lowers the reaction temperatures. Differential thermal analysis found endotherms at 1050 and 1110 °C with sintered $NiCr/ZrO_2$ powders, and at 980 and 1100 °C when pre-oxidized powders were used. These are shown to be associated with local melting at the metal/ceramic interface. This thus explains the existence of a critical bonding temperature for good-quality diffusion bonding, where a minimum temperature has to be satisfied for the eutectic reaction to occur.

## 1. Introduction

There have been a number of joining techniques developed and improved for the joining of metal and ceramics, e.g. mechanical joining, brazing and diffusion bonding [1]. These techniques have potential applications in the areas of electronics and sensors, aerospace, car and nuclear industries, and are expected to continue and develop. Among these techniques, diffusion bonding offers advantages for high-temperature applications, as it is a solid state process, performed at elevated temperatures (typically 0.6–0.8 of the least refractory of the materials to be joined), which introduces a minimum of microstructural damage.

The qualities of metal/ceramic diffusion bonds largely depend on the interface properties, both chemical and physical. If there is no chemical reaction at the metal/ceramic interface, an inherent affinity or wettability coupled with a small thermal expansion mismatch of the joining materials is important for a good joint. In the case of a large thermal expansion mismatch or poor wettability, an interlayer or multi-interlayer bond is normally employed, so that a low thermal expansion mismatch and good interface affinity can be realized at each interface [2–4]. However, if there is a reaction at the interface, the reaction layer can play a major role in both the diffusion-bonding process and the subsequent properties of the joints. In the limiting case, reactions can lead to interfacial melting, such as is found during diffusion bonding of $Pd/ZrO_2$[5–6]. In this case, the reaction makes diffusion bonding similar to brazing [7]. This kind of eutectic reaction layer may work as a bridge of intermediate properties between dissimilar materials and so may solve the problem of larger differences in thermal expansion coefficient and improve the wettability at the metal/ceramic interface. It is also known that vigorous reactions between metal and ceramic components during bonding do not necessarily make good joints, e.g. Ni/SiC [8]. In this case the thick intermetallic reaction layer is probably too brittle. Thus for metal/ceramic diffusion bonding, much further research needs to be carried out on interface behaviour. Furthermore, an understanding of interfaces will also benefit studies in related areas such as metal-matrix ceramic composites, where the interface is important in determining the overall properties of the material [9–10].

Here an investigation into the diffusion bonding of a Ni(Cr) alloy to TZP $ZrO_2$ is presented. $ZrO_2$ was used because of its many potential applications due to its high toughness. The use of a Ni(Cr) alloy is to allow comparison with previous work on the diffusion bonding of $Ni/ZrO_2$ [11–13] and act as a model for the behaviour of more complex high-temperature alloys.

## 2. Experimental procedure

Ni(Cr) (80:20 at %) foils of thickness 125 μm (Goodfellow Metals) were used. Some of these were pre-oxidized in air for 2 h at 900 °C forming a layer of oxides with a thickness of about 1 μm (denoted NiCr(O)). Yttria-stabilized TZP zirconia cylinders

(Dynamic Ceramic, UK) of diameter 15 mm and length 14 mm, were cut using a diamond saw. One surface was lapped flat and polished using a 3 µm diamond paste as a final polish. Two $ZrO_2$ cylinders were assembled around one foil in a sandwich configuration (ceramic/metal/ceramic) before inserting into diffusion bonder. Diffusion bonds were made at 1100 °C under a contact pressure of 10 MPa in a vacuum of $10^{-3}$ mbar for times of 10–360 min. Specimens of size 2 mm × 2 mm × 28 mm were cut from the diffusion-bonded sandwiches for four-point bend testing. Some of these specimens were annealed in either air or vacuum at a temperature of 1100 °C for 1 h prior to testing. About four specimens were used to calculate the mean modulus of rupture from the four-point bond test results. Cross-sections and fractured halves of the interfaces were investigated by optical microscopy, together with some chemical etching of the cross-sections by a solution of $1HNO_3$ + 1alcohol + $1H_2O$. Scanning electron microscopy and X-ray composition microanalysis (electron probe microanalysis) were also carried out.

In order to facilitate preparation and to increase the chance of achieving a thin area at the metal/ceramic interface for transmission electron microscopy studies, multilayer diffusion bonds were fabricated. In this case, 200 µm thick slices were cut from the $ZrO_2$ stock and lapped flat. A number of these were stacked with NiCr(O) foil and bonded under the same conditions as were used for the sandwich specimens. The bonded multilayers were cut into 200 µm slices which were dimpled and ion-beam thinned to perforation. A Philips CM20 microscope was used to examine the interfaces.

Various well-mixed powders of $ZrO_2$ and Ni, Cr, Ni/Cr alloys (Goodfellow Metals), some of which were pre-oxidized at 900 °C for 12 h in air, were compressed, respectively, under conditions identical to the diffusion bonding at 1100 °C for 1 h under a pressure of 10 MPa to produce equivalent multi-interface specimens for differential thermal analysis (DTA) studies of interface reactions.

## 3. Results

### 3.1. Bond mechanical properties

The bonding strengths measured are tabulated in Table I. Diffusion bonds of $Cr/ZrO_2$ did not show any measurable strength. The strength of $Ni/ZrO_2$ diffusion bonds reported in a previous work [13] are listed for comparison. $NiCr/ZrO_2$ and $NiCr(O)/ZrO_2$ diffusion bonds show low strength if the bonding temperature is below 1100 °C, for example at 1000 °C. Thus only diffusion bonds made at 1100 °C were fabricated for a range of bonding times. These diffusion bonds showed an increase in strength with increasing time at the bonding conditions; however, when the bonding time reaches 2 h, the bond strength approaches the strength of the ceramic, with subsequent fracture occurring normally in the zirconia. In general, the strength of the bonds of pre-oxidized $NiCr(O)/ZrO_2$ are stronger than those of $NiCr/ZrO_2$. Annealing in vacuum reduces the bond strength more than annealing in air. It is also notable that the bond strengths of $NiCr(O)/ZrO_2$ and $NiCr/ZrO_2$ have similar values for any common annealing heat treatment.

### 3.2. Microstructures of the interfaces

No interface reactions were observed with $Cr/ZrO_2$ diffusion bonds fabricated at 1100 °C for 1 h. Fig. 1 shows diffusion bonds of both $NiCr/ZrO_2$ and $NiCr(O)/ZrO_2$ made at 900 °C, no obvious reaction was seen even when the diffusion bonding time was 3 h. However, when bonding pre-oxidized $NiCr(O)/ZrO_2$, nickel and/or chromium oxide underwent reduction where it was in contact with $ZrO_2$; this is seen as bright zones in Fig. 1b. This is similar behaviour to our previous findings with the diffusion bonding of pre-oxidized $Ni/ZrO_2$ [13]. However, above this diffusion-bonding temperature, e.g. bonds made at 1000 °C for 3 h, traces of reaction products could be seen on the fracture surfaces of broken bonds (shown in Fig. 2). In general, the reaction between NiCr(O) and $ZrO_2$ was more vigorous than that between NiCr and $ZrO_2$. In Fig. 3, reaction products on the exposed metal fracture surfaces are shown

TABLE I Modulus of rupture of diffusion bonds between various metals and zirconia made under a pressure of 10 MPa in a vacuum of $10^{-3}$ mbar

| Specimen (foil composition) | Temperature (°C) | Time (min) | Strength (MPa) | | |
|---|---|---|---|---|---|
| | | | As-bonded | Annealed in vacuum | Annealed in air |
| Ni [13] | 1100 | 60 | 38 ± 14 | 36 ± 3 | 63 ± 2 |
| Cr | 1100 | 60 | 0 | 0 | 0 |
| NiCr | 1100 | 30 | 250 ± 38 | | |
| | | 60 | 397 ± 91 | 86 ± 9 | 161 ± 32 |
| | | 120 | 574 ± 27 | 74 ± 12 | 223 ± 12 |
| | 1000 | 60 | 70 ± 40 | | |
| NiCr(O) | 1100 | 10 | 220 ± 23 | | |
| | | 30 | 260 ± 41 | | |
| | | 60 | 420 ± 21 | 60 ± 20 | 169 ± 15 |
| | | 120 | 620 ± 41[a] | 66 ± 5 | 241 ± 91 |
| | 1000 | 60 | 105 ± 46 | | |

[a] This strength is for $ZrO_2$ because fracture occurred away from the interface, ie., in the $ZrO_2$ bulk.

from diffusion bonds of both NiCr/$ZrO_2$ and NiCr(O)/$ZrO_2$ made at 1100 °C for only 1 h. Fig. 4 shows the morphology of the ceramic halves, which correspond to the reaction products seen on the metal halves shown in Fig. 3. Diffusion bonds of NiCr(O)/$ZrO_2$ made at 1200 °C for 6 h further confirm that reactions occur at the metal/ceramic interface. Fig. 5 is a cross-sectional view showing that the ceramic seems to have partially dissolved and thus small regions of $ZrO_2$ protrude into the metal. This microstructure is believed to be the result of liquid reaction products which have been extruded from the interface by the bonding pressure. The ceramic regions and the metal were analysed by EPMA as $(Ni_{0.4}Cr_{0.1}O_4)(ZrO_2)$ and $(Zr_{0.3}O_{1.5})$ $(Ni_{3.6}Cr)$, respectively. Reaction products form after very short bonding times; Fig. 6 shows the metal fracture surface of a NiCr/$ZrO_2$ bond fabricated at 1100 °C for 10 min, a faint decoration of a dendritic structure indicates interfacial melting followed by resolidification. Very similar structures were seen in earlier studies of Pd/$ZrO_2$ diffusion bonds [5,6] where interdiffusion at the interface leads to a eutectic reaction. For the diffusion bonds of NiCr(O)/$ZrO_2$ made at 1100 °C for 10 min, the morphology of the reaction products was seen to be similar to that made for 1 h, though the amount of reaction product was less.

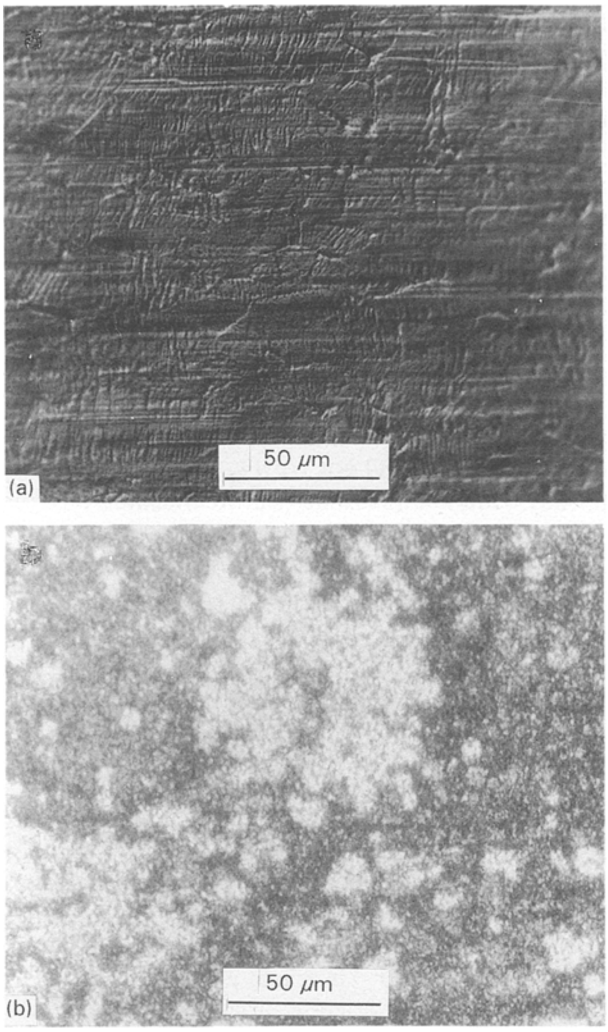

*Figure 1* Optical micrographs of metal halves of fractured diffusion bonds made at 900 °C for 3 h. (a) NiCr foil, the extrusion line traces are visible indicating no chemical reaction occurred. (b) NiCr(O) foil, bright regions represent areas where the oxides were reduced, the dark areas are the original oxidized surface morphology.

Annealing of the diffusion bonds was performed in order to study the chemical properties of the reaction layer and the stability of the bonds under annealing conditions. Annealing in both air and vacuum changes the microstructures of these interface interphases. In Figs 7 and 8 annealing in vacuum is seen to destroy those phases progressively, starting from the specimen edges. As the reduction of the reaction products starts from the specimen edges, some residue of the original phases are still seen in central areas. For annealing in air, oxidation of the interface interphases occurred.

Cross-sections revealed that finer grains were developed after oxidation of the Ni(Cr) alloy (Fig. 9). EDX qualitative composition microanalysis showed that the grain boundaries in the metal foil of the bonds of NiCr(O)/$ZrO_2$, are chromium-rich. For diffusion bonding of NiCr(O)/$ZrO_2$, a reaction layer of about 1 μm thickness was found by SEM (Fig. 10). Cross-sectional TEM of the interface of NiCr(O)/$ZrO_2$ fabricated at 1100 °C for 1 h under a pressure of 10 MPa

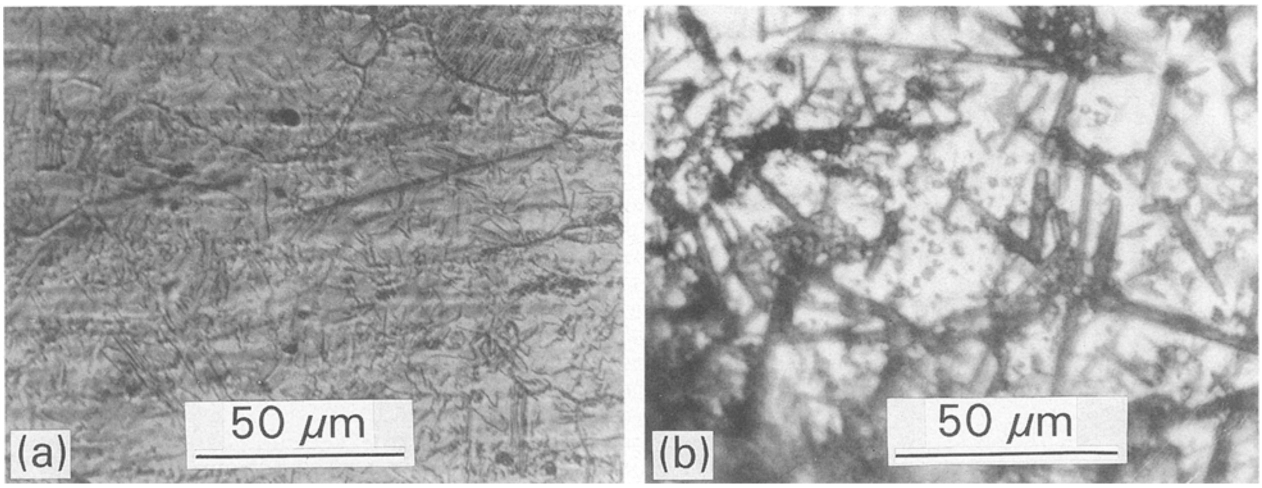

*Figure 2* Optical micrograph of metal halves of fractured diffusion bonds made at 1000 °C for 3 h. (a) NiCr foil, traces of reaction products of dendritic form are visible. (b) NiCr(O) foil, reaction products of needle-like form are seen at the foil surface.

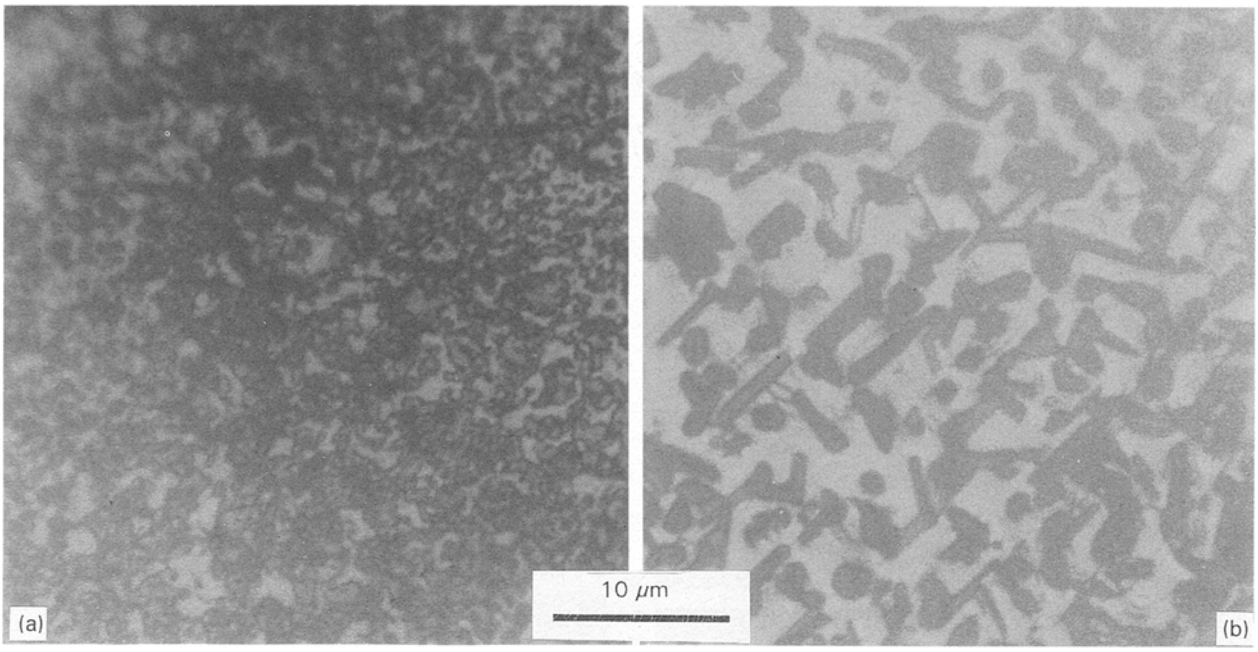

*Figure 3* Optical micrograph of metal halves of fractured diffusion bonds made at 1100 °C for 1 h. (a) NiCr foil, (b) NiCr(O) foil. Note the reaction products over the interface exposed on the fracture surface.

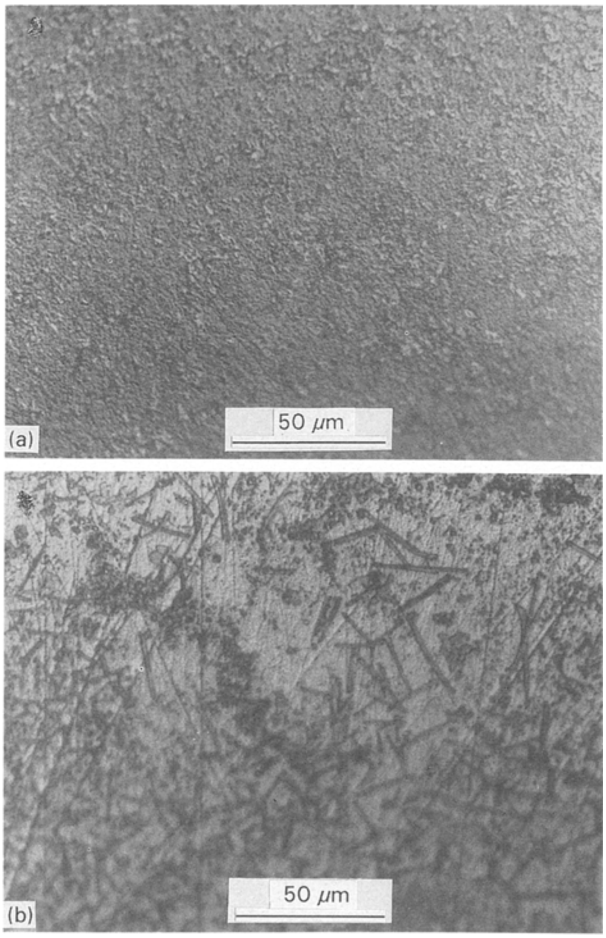

*Figure 4* Optical micrograph of ceramic halves of fractured diffusion bonds made at 1100 °C for 1 h. (a) The dissolution or corrosion of the ceramic surface is apparent from when the ceramic was diffusion bonded to NiCr. (b) Residual reaction products can be observed when diffusion bonded to NiCr(O).

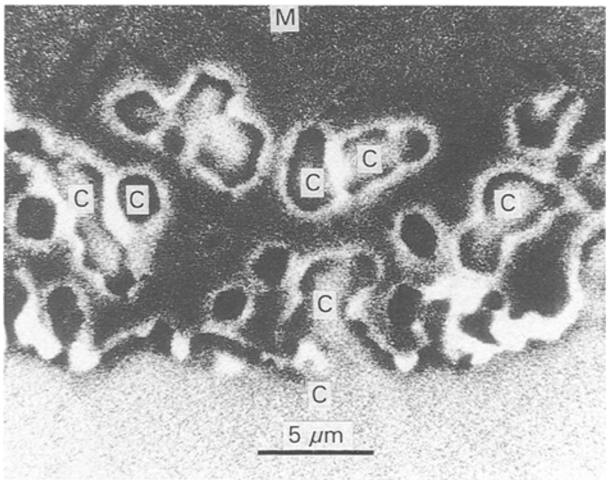

*Figure 5* Back-scattered electron scanning electron micrograph of the cross-section of NiCr(O)/$ZrO_2$ diffusion bond made at 1200 °C for 6 h. Note the regions of the ceramic (marked C) in the metal (marked M).

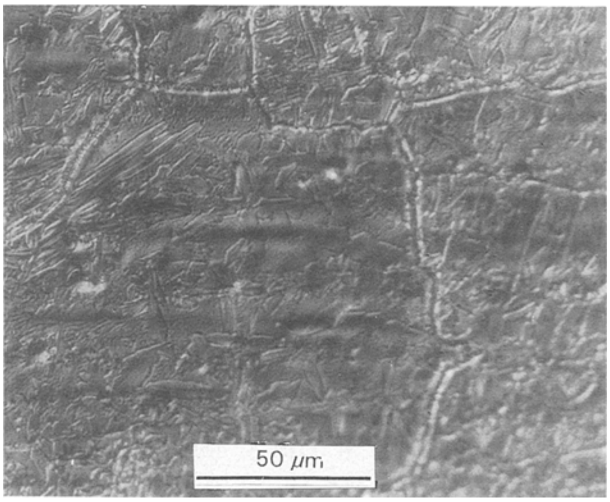

*Figure 6* Optical micrograph of the reaction products showing a faint dendritic structure, from the early stages of the reaction, seen on the metal fracture halves of a NiCr foil diffusion bonded at 1100 °C for 10 min.

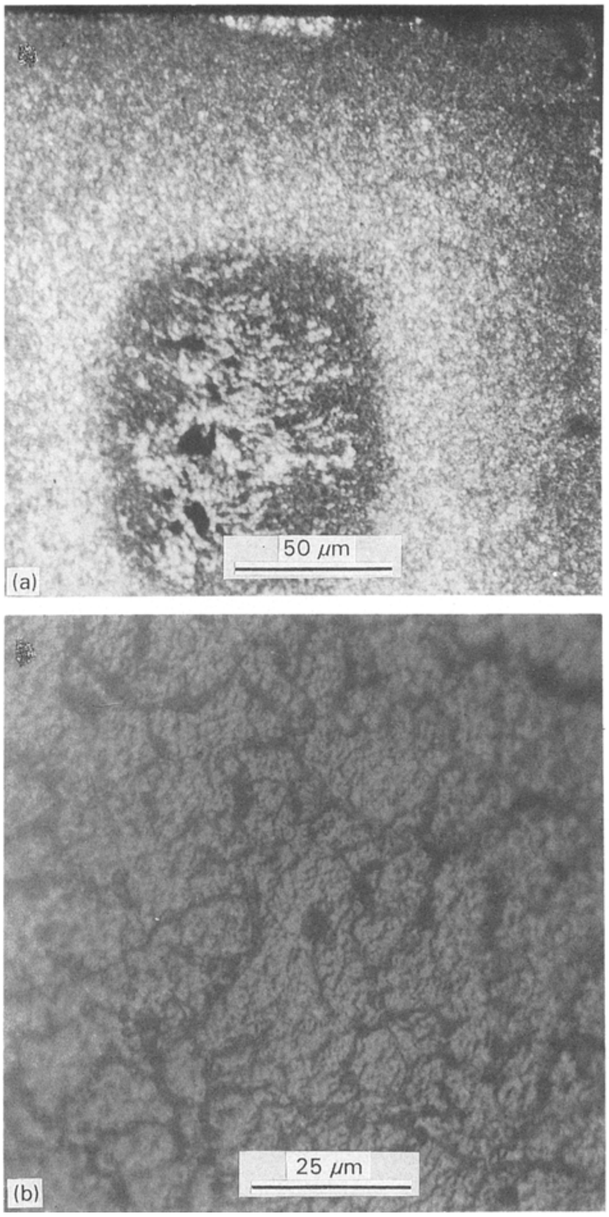

*Figure 7* Optical micrograph of the interface microstructures from fractured diffusion bonds of NiCr/$ZrO_2$ fabricated at 1100 °C after annealing in vacuum for a further hour at 1100 °C. (a) The morphology of the original reaction products was changed and the central area retained the original microstructure to some extent. (b) Higher magnification shows that the original reaction products disappeared.

shows that the reaction products form as layers (Fig. 11), which fracture under electron-beam heating. Assuming a spinel structure, the lattice parameter of the reaction products is determined to be 0.565 nm (Fig. 12) by diffraction analysis.

Quantitative composition microanalysis using a Cameca electron microprobe equipped with WDX detection shows that the interface layer is chromium- and oxygen-rich for both diffusion-bonding NiCr(O)/$ZrO_2$ made at 1100 °C for 1 h and NiCr/$ZrO_2$ made at 1200 °C for 6 h; a typical result is shown in Fig. 13 for NiCr(O)/$ZrO_2$, as an example; however, no detectable segregation of chromium and/or oxygen was found at the interface of NiCr/$ZrO_2$ diffusion bonds made at 1100 °C for 1 h.

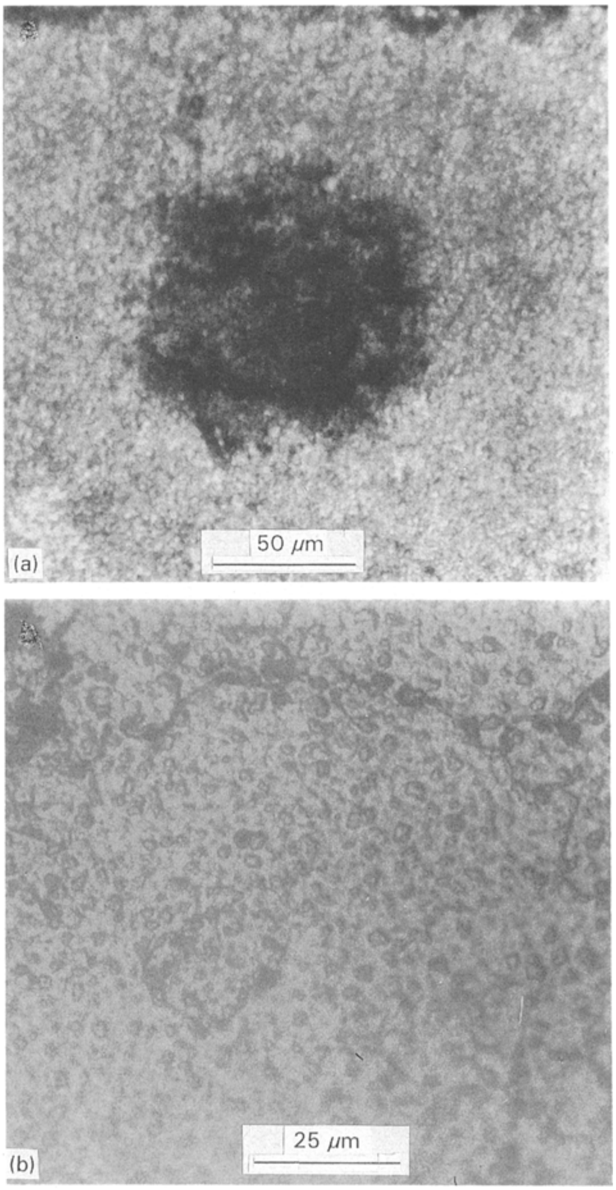

*Figure 8* Optical micrograph of the metal halves of NiCr(O)/$ZrO_2$ bonds fabricated at 1100 °C after annealing in vacuum for 1 h at 1100 °C. (a) Note the contrast difference of the specimen edges and the centre. The central dark region retains the original morphology of the reaction products. The bright area, seen in (b), results from the reduction of the reaction products at the interface.

### 3.3. Differential thermal analysis (DTA)

DTA was carried out on different powder mixtures of nickel, chromium, $ZrO_2$, as listed in Table II, so that reactions between certain powders can be distinguished from others. These powder mixtures were hot pressed to promote interdiffusion reactions before DTA was carried out. The NiO and $Cr_2O_3$ were made by oxidizing the pure nickel and chromium powders. The endotherms were detected only for the mixtures of nickel, chromium and $ZrO_2$ at 1050 and 1110 °C, and the mixtures of NiO, $Cr_2O_3$ and $ZrO_2$ at 980 and 1100 °C, as shown in Fig. 14.

## 4. Discussion

For diffusion bonding of Pd/$ZrO_2$ [5, 6] a critical diffusion-bonding temperature was found at about 1050 °C; below this temperature no good bonding is

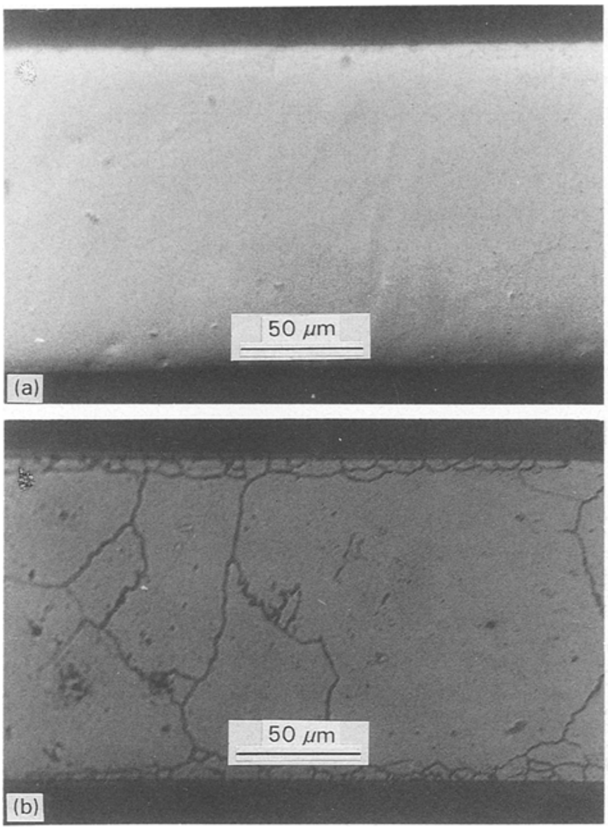

*Figure 9* Optical micrograph of a cross-sectional view of a diffusion bond made at 1100 °C for 1 h after chemical etching. (a) $NiCr/ZrO_2$ diffusion bonds, no grain boundaries can be seen in the metal foil. (b) Grain boundaries seen clearly in a pre-oxidized NiCr foil. A thin layer of fine grains has been produced on top of the metal foil.

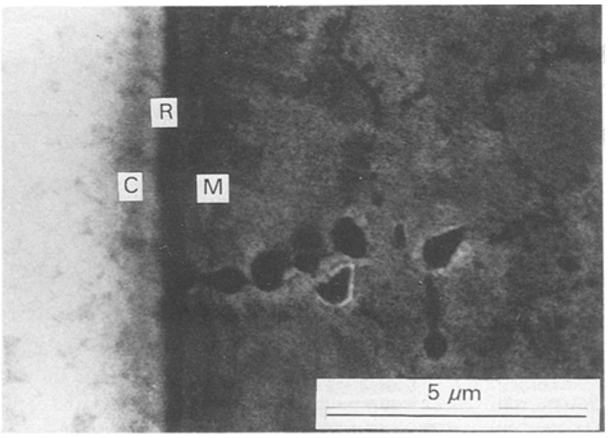

*Figure 10* Scanning electron micrograph showing a dark contrast reaction layer at the interface of $NiCr(O)/ZrO_2$ made at 1100 °C and 1 h. C, M and R represent ceramic, metal and reaction layer, respectively.

*Figure 11* A bright field transmission electron micrograph of the interface microstructure of the diffusion bonds of $NiCr(O)/ZrO_2$ made at 1100 °C for 1 h under a pressure of 10 MPa. The reaction layer is seen as bands fractured mainly parallel to the interface.

possible. This is believed to be because the diffusion bonding is controlled by a eutectic reaction at about 1030 °C, which promotes the wetting of the metal/ceramic pairs and eliminates interface defects effectively. In the present study, similar behaviour was observed for diffusion bonding of $NiCr/ZrO_2$ with the critical temperature at 1050 °C. Pre-oxidizing the metal foil lowers this critical temperature to 980 °C. These critical temperatures were determined by DTA and correspond to the observed interface microstructure change with a small error (50 °C). Reaction products were only seen with diffusion bonds of $NiCr/ZrO_2$ and $NiCr(O)/ZrO_2$ above 1000 °C (Fig. 2).

However, by DTA, there are two clear endotherms detected for both $NiCr/ZrO_2$ and $NiCr(O)/ZrO_2$. This fact may correspond to two types of reaction product, which cannot be distinguished in this study. As the reaction between $NiCr/ZrO_2$ is not as vigorous as the reaction between $NiCr(O)/ZrO_2$, the reaction layer can only be examined by cross-sectional analysis for $NiCr(O)/ZrO_2$ (Figs 9 and 10). As all DTA was carried out after hot-pressing for 1 h the endotherms possibly represent the melting of interface reaction products.

Nickel, chromium and oxygen can form a spinel phase ($NiCr_2O_4$) and other mixed compounds at elevated temperatures above 1000 °C as determined by Thomassen [14], and above 850 °C as determined by Muller *et al.* [15]. These were studied here by annealing the NiCr foil and the oxidized foil of NiCr(O) in vacuum at 1100 °C for 1 h and then examining by SEM. Fig. 15 shows that nickel, chromium and oxygen compounds were formed at the foil surfaces. This compound formation was either insignificant or was a continuous process for the powder mixtures of nickel and chromium and NiO and $Cr_2O_3$, thus DTA (see Table II) did not detect the endotherms for such compound formation. The reaction products seen at the interfaces are not only these nickel, chromium and oxygen compounds because the

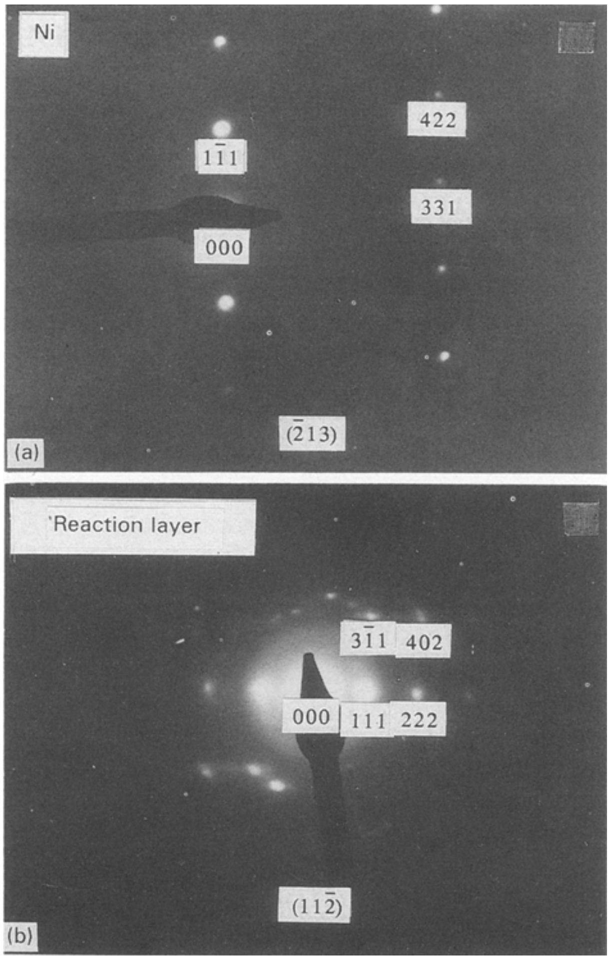

*Figure 12* Electron diffraction analysis shows that the lattice parameter is 0.565 nm for the reaction product (b) (if it is assumed to be of spinel structure). Diffraction from the nickel foil (lattice parameter 0.35 nm) attached to the reaction layer was used as reference (a).

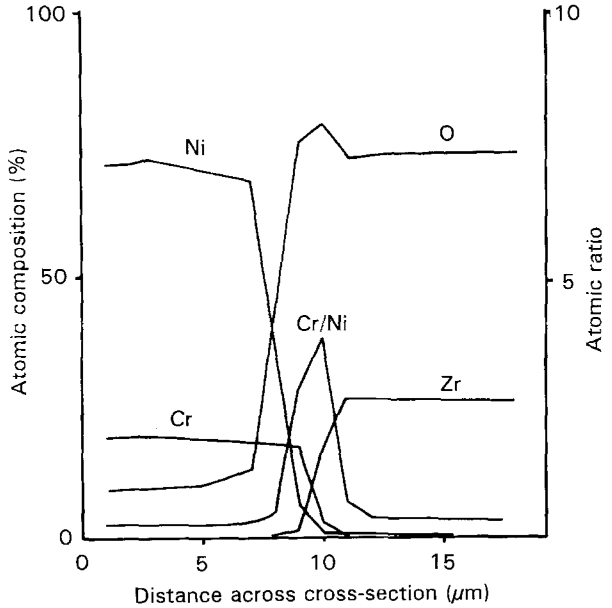

*Figure 13* WDX microanalysis across the cross-section of NiCr(O)/$ZrO_2$ diffusion bond made at 1100 °C for 1 h, the Cr/Ni ratio plot shows that the chromium concentration is enhanced at the interface. Oxygen segregation at the interface is also apparent.

TABLE II List of powder mixtures and the endotherms detected by DTA in temperature range 20–1300 °C.

| Powders | Endotherms |
|---|---|
| Ni | No |
| Cr | No |
| Ni + Cr | No |
| $NiO + Cr_2O_3$ | No |
| $Ni + ZrO_2$ | No |
| $Cr + ZrO_2$ | No |
| $NiO + ZrO_2$ | No |
| $Cr_2O_3 + ZrO_2$ | No |
| $Ni + Cr + ZrO_2$ | 1050 and 1110 °C |
| $NiO + Cr_2O_3 + ZrO_2$ | 980 and 1100 °C |

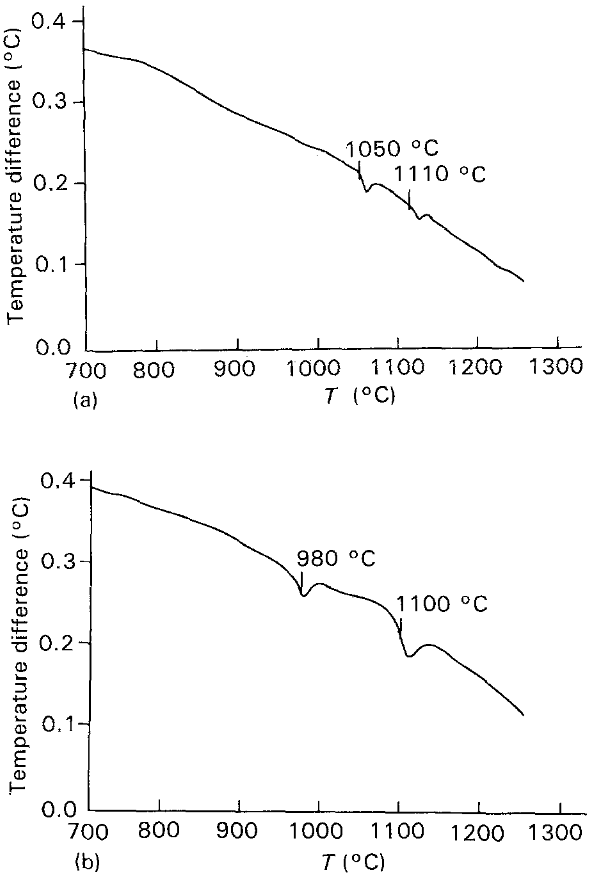

*Figure 14* DTA of powder mixtures fabricated at 1100 °C under a pressure of 10 MPa for 1 h. (a) Nickel, chromium and $ZrO_2$ powder mixture. (b) Nickel, chromium pre-oxidized powders and $ZrO_2$ powder mixture. Note each diagram shows two endotherm peaks.

dissolution of $ZrO_2$ is evident in Fig. 4. At the interface of NiCr/$ZrO_2$, oxygen and zirconium components of the ceramic may diffuse into the metal and form complex compounds and low melting point eutectic phases. In the case of NiCr(O)/$ZrO_2$, the extra oxygen element in the surface layer of the metal foil may favour the above reactions, hence the reaction temperatures are lowered. In an X-ray diffraction study of the $NiO–Cr_2O_3–ZrO_2$ system made by a mixture of oxide gels [16], chromium oxidation was retarded by the presence of other oxides, for instance by the formation of an oxide of chromium intermediate between $Cr_2O_3$ and $CrO_3$. However, the

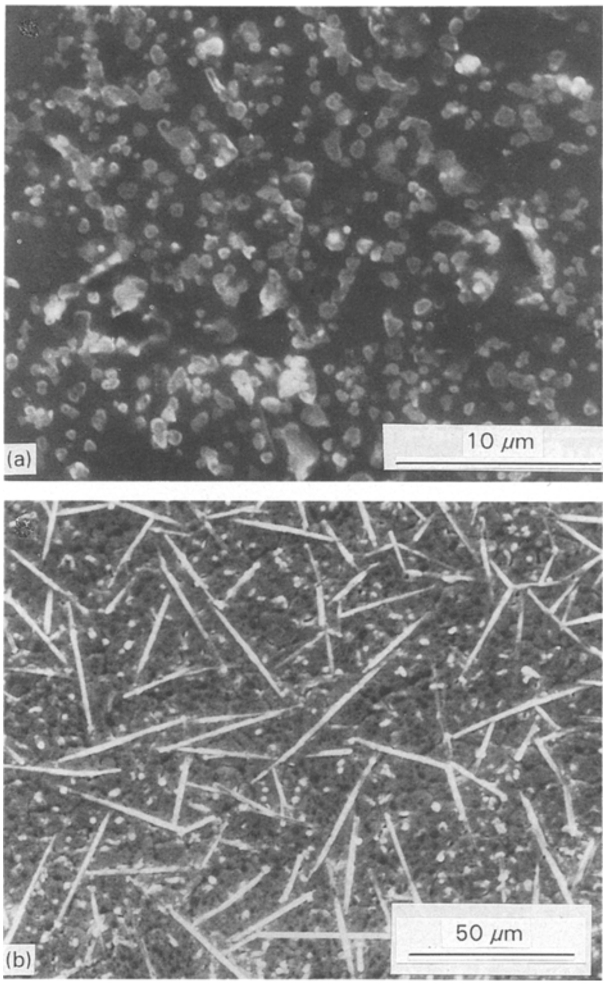

*Figure 15* Scanning electron micrograph of the annealed NiCr and NiCr(O) foils. (a) Segregation of chromium from the nickel base or formation of compounds of nickel, chromium and oxygen in the vacuum is obvious. (b) Formation of a compound in needle-like form, possibly the spinel $NiCr_2O_4$ , is shown.

present results cannot confirm this, and instead may indicate the formation of a new spinel compound, for example, $NiO_{1-x}Cr_2O_{3-y}ZrO_{2-z}$ $(0 < x, y, z < 1)$ with a lattice parameter of 0.565 nm.

Thus the diffusion bonding of $NiCr/ZrO_2$ is controlled by an interface chemical reaction, possibly similar to the eutectic reaction observed with $Pd/ZrO_2$ [5, 6]. It is postulated that the reaction products should be a eutectic resulting in a ternary oxide of mean composition $NiO_{1-x}Cr_2O_{3-y}ZrO_{2-z}$ $(0 < x, y, z < 1)$, as any combination of the two oxides does not give rise to any endotherm. For diffusion bonding of $NiCr(O)/ZrO_2$ a thicker reaction layer can be found (Fig. 10). Furthermore, the presence of oxygen also lowers the DTA endotherms. These indicate that the presence of oxygen may favour the formation of these interface reactions, in contrast to the $Pd/ZrO_2$ bonds, where the eutectic reaction only occurs at low oxygen partial pressures. Annealing in vacuum should reduce the oxygen from the reaction products, and may destabilize the products, as shown in Fig. 8. Tensile stresses concentrated at the specimen edges may also play a role in reducing the bonding strength by generating voids at the edges, as analysed by Cao *et al.* [17] and shown by Qin and Derby [13]. The mechanism by which annealing in air decreases the bond strength is not certain. It may be by destabilizing the reaction products because of oversaturation of oxygen, or by generating mismatch stresses at the specimen edges due to the formation of a layer of oxides evolving from the surfaces of the specimen. For example, for the reaction of

$$Ni + 1/2O_2 \rightarrow NiO \qquad (1)$$

a 100% volume expansion is expected. If oversaturation of oxygen destabilizes the reaction products, the original strong bonding by the chemical bridging of the reaction layer will be removed. Also, if a volume expansion of the metal alloy foil occurs close to the specimen edges by oxidation, higher residual stresses will be generated. Existing voids may be filled up by this volume expansion in contrast to the generation of new voids from annealing in vacuum [13]. Both will affect bond strength adversely. However, annealing in air reduces the bonding strength less than annealing in vacuum. This probably means that nickel and chromium oxides have a better adhesion than nickel or chromium to $ZrO_2$ and agrees with the analysis that oxides have a better adhesion to oxides than oxides to metals [18]. Such a phenomenon has also been noticed in a previous work on diffusion bonding of $Ni/ZrO_2$ where annealing $Ni/ZrO_2$ bonds in air improves bonding strength [14] and $NiO/ZrO_2$ gives rise to a stronger bonding than that of $Ni/ZrO_2$ [11–13].

## 5. Conclusions

Good diffusion bonds of $NiCr/ZrO_2$ can only be made above a critical temperature of 1050 °C, when there is a strong eutectic reaction at the interface. The reaction is necessary to promote strong interface adhesion and good mechanical strength of the subsequent joints. The presence of oxygen enhances the reaction and lowers the eutectic temperature, hence pre-oxidizing the Ni(Cr) alloy enhances bonding strength dramatically. It is postulated that the reaction products are in a form of $NiO_{1-x}Cr_2O_{3-y}ZrO_{2-z}$ $(0 < x, y, z < 1)$ spinel with a lattice parameter of 0.565 nm, which dissolves in an atmosphere of low oxygen partial pressure. This counter-reaction process explains why the bonds weaken after annealing in vacuum. The negative effects of annealing in air on bond strength are not yet understood. Possibly a vigorous oxidization of the metal alloy foil makes the foil volume increase near the specimen edges, thus generating high mismatch stresses over the whole interface; or possibly oversaturation of the oxygen atmosphere during annealing conditions destabilizes the reaction products

## Acknowledgements

The authors thank Mr. C. Salter for the help with X-ray analysis. The research was funded by the SERC grant GR/E 76742.

## References

1. M. G. NICHOLAS and D. A. MORTIMER, *Mater. Sci. Technol.* **1** (1985) 657.
2. K. SUGANUMA, T. OKAMOTO, M. KOIZUMI and M. SHIMADA, *J. Mater. Sci.* **22** (1987) 1359.
3. J. T. KLOMP, *Am. Ceram. Soc. Bull.* **51** (1972) 683.
4. M. G. NICHOLAS and R. M. CRISPIN, *J. Mater. Sci.* **17** (1982) 3347.
5. C-D. QIN and B. DERBY, in "Diffusion Bonding 2", edited by D. J. Stephenson, Proceedings of the 2nd International Conference on Diffusion Bonding (Elesevier, 1991) p. 224.
6. *Idem, Acta Metall. Mater.* **40** (1992) 925.
7. R. E. LOEHMAN and A. P. TOMSIA, *Am. Ceram. Soc. Bull.* **67** (1988) 375.
8. T. C. CHOU, A. JOSHI and J. WADSWORTH, *J. Mater. Res.* **6** (1991) 796.
9. R. WARREN and C-H. ANDERSSON, *Composites* **15** (1984) 101.
10. M. RUHLE and A. G. EVANS, *Mater. Sci. Eng.* **A107** (1989) 187.
11. YAMANE, Y. MINAMINO, K. HIRAO and H. OHNISHI, *J. Mater. Sci.* **21** (1986) 4227.
12. J. G. DUH and W. S. CHIEN, *ibid.* **25** (1990) 1529.
13. C-D. QIN and B. DERBY, *J. Mater. Res.* **7** (1992) 1480.
14. L. THOMASSEN, *J. Am. Ceram. Soc.* **62** (1940) 1134.
15. O. MULLER, R. ROY and W. B. WHITE, *ibid.* **51** (1968) 693.
16. W.O. MILLIGAN and L. M. WATT, *J. Phys. Colloid Chem.* **52** (1948) 203.
17. H. C. CAO, M. D. THOULESS and A. G. EVANS, *Acta Metall.* **36** (1988) 2037.
18. A. M. STONEHAM and P. W. TASKER, *Mater. Sci. Res.* **21** (1987) 155.

*Received 10 March 1992*
*and accepted 15 January 1993*